

# Assessment of Walking Features From Foot Inertial Sensing

Angelo M. Sabatini\*, *Member, IEEE*, Chiara Martelloni, Sergio Scapellato, and Filippo Cavallo

**Abstract**—An ambulatory monitoring system is developed for the estimation of spatio-temporal gait parameters. The inertial measurement unit embedded in the system is composed of one bi-axial accelerometer and one rate gyroscope, and it reconstructs the sagittal trajectory of a sensed point on the instep of the foot. A gait phase segmentation procedure is devised to determine temporal gait parameters, including stride time and relative stance; the procedure allows to define the time intervals needed for carrying an efficient implementation of the strapdown integration, which allows to estimate stride length, walking speed, and incline. The measurement accuracy of walking speed and inclines assessments is evaluated by experiments carried on adult healthy subjects walking on a motorized treadmill. Root-mean-square errors less than 0.18 km/h (speed) and 1.52% (incline) are obtained for tested speeds and inclines varying in the intervals [3, 6] km/h and [−5, +15]%, respectively. Based on the results of these experiments, it is concluded that foot inertial sensing is a promising tool for the reliable identification of subsequent gait cycles and the accurate assessment of walking speed and incline.

**Index Terms**—Ambulatory measurements, gait analysis, inertial sensing, uphill and downhill walking.

## I. INTRODUCTION

THE TRADITIONAL approach to quantitative motion analysis has proven to be clinically very useful, in spite of the fact that the implementation can be critical. First, traditional motion analysis systems are quite expensive and difficult to be operated. Second, only a limited capture volume is allowed, which limits, e.g., the number of consecutive gait strides that can be acquired. Third, these systems must operate in controlled environments, which hinders them from gathering information about the extent subjects perform functional activities outside the laboratory setting. These are some reasons behind the recent surge of interest in ambulatory monitoring systems [1]–[5]. In this context, either used alone or combined with other sensing devices, inertial sensors (accelerometers and rate gyroscopes) are becoming increasingly popular, due to their low cost, small size, light weight, and limited power requirements.

Recently, a number of papers have been published with the purpose of demonstrating that either accelerometers or gyroscopes can be used to detect simple temporal or spatial features of gait. Temporal features of gait, such as the stride time, can be

detected by heel [6], thigh [7], and waist [8] accelerometry; heel [2], thigh [9], and combinations of thigh and shank gyroscopy [10], [11]. Generally, the estimation algorithms detect invariant signal features, such as the sharp peaks occurring when the foot hits the ground. When the sensors are placed on both legs, it is possible to analyze the step time and gait symmetry. Mostly, the connection with spatial gait features, such as the stride length, is by indirect methods. For instance, the reconstructed angular rotations of body segments relative to the absolute space—the thigh, [9]; the thigh and the shank, [11]—are entered in simple and double segment gait models. An indirect method of analysis based on the parameterization of trunk and heel accelerations, combined with the use of artificial neural networks, allows to estimate the walking speed and the incline [6]; standard regression tools are used to characterize the relationship between the root mean square norm of the acceleration vector and the walking speed [12]. The limitation of most indirect methods is that, due to the effects of physiological variability on the model accuracy, frequent subject-per-subject calibration procedures are needed, which may require additional sensors [12], [13].

The alternative to indirect methods is double-integration of the accelerometric signals [14]—a difficult task in practice, since the initial conditions of position and velocity are uncertain, and the orientation-dependent gravitational component must be separated from the acceleration of the sensed anatomical point. Accelerometric systems have been proposed to estimate the position/orientation of body segments in the three dimensional (3-D) space by using multiple accelerometers to calculate the relative angle between two joints [15], [16]. Inertial sensing has several advantages: the attachment of gyroscopes to the body segments is easier compared with accelerometers, gyroscopes are insensitive to the influence of gravity, the joint angle information is obtained by using only one gyroscope [17], [18]; additionally, spatial gait parameters can be estimated by direct methods based on strapdown integration [19], once the initial conditions are obtained by exploiting the cyclical properties of human walking [15].

The ambulatory monitoring system described in this paper is for reconstructing the sagittal position/orientation of a single body part, i.e., the instep of the foot. It can estimate a number of temporal gait parameters, i.e., the stride time and the relative stance, and spatial gait parameters, i.e., the stride length. Beside the walking speed, the incline can also be estimated. We are aware of two previous approaches to foot inertial sensing. Veltink *et al.* [20] describe a 3-D foot inertial sensing system, embedded in a two-channel implantable foot-drop stimulator; their main interest is the assessment of the system sensitivity to measure the influence of stimulation levels on the foot

Manuscript received November 5, 2003; revised July 2, 2004. This work was supported in part by a grant from the Fondazione Cassa di Risparmio di Pisa, Italy (Kid-rollbot project), and in part by the Italian Ministry of University and Research (Fondi di Ricerca di Ateneo). *Asterisk indicates corresponding author.*

\*A. M. Sabatini is with the Scuola Superiore Sant'Anna, Piazza Martiri della Libertà 33, 56127 Pisa, Italy (e-mail: A.Sabatini@mail-arts.sssup.it).

C. Martelloni, S. Scapellato, and F. Cavallo are with the Scuola Superiore Sant'Anna, 56127 Pisa, Italy.

Digital Object Identifier 10.1109/TBME.2004.840727

movements of drop-foot patients; no actual measurements are demonstrated in terms of assessment of walking features such as walking speed and incline. Sagawa *et al.* [21] describe an application where the travelled distance is estimated during level walking; seemingly, they did not fully investigate how their system performs in different walking conditions [22]. In this paper, we characterize the accuracy of the foot inertial sensing approach in assessing the walking speed and the incline by conducting treadmill walking trials at several controlled combinations of speed and incline values.

## II. METHOD

### A. Experimental Instrumentation

The inertial measurement unit (IMU) was composed of one biaxial accelerometer (Analog Devices ADXL210E) and one rate gyroscope (Murata ENC-03J). The accelerometer is endowed with silicon resistors whose electrical resistance changes in response to the applied mechanical load. The resistors are electrically connected in a Wheatstone bridge to produce a voltage proportional to the acceleration of the small mass in the sensor. The gyroscope is endowed with a vibrating element—an oscillating piezoelectric bimorph. The principle of operation is the measurement of the Coriolis acceleration which is generated when a rotational angular velocity is applied to the vibrating element.

Before sampling, the accelerometer and gyroscope signals were single-stage low-pass filtered at 50 Hz and amplified; the gyroscope sensitivity was  $2.5 \text{ mV}/^\circ/\text{s}$ . 12-bit sampling was performed at  $f_s = 200 \text{ Hz}$  ( $T_s = 5 \text{ ms}$ ) using a PCMCIA card (National Instruments (NI) DAQ card-6062E); this card was controlled by NI's LabView v. 6.1 software, for data acquisition and storage. The accelerometer calibration was performed by placing its sensitive axes in line with gravity, when the nominal output is  $+1 g$  and  $-1 g$  ( $g = 9.81 \text{ m/s}^2$  is the gravitational acceleration). The gyroscope calibration consisted of imparting a known rotation ( $+90^\circ$ ) to the case containing the sensor; the gyroscope signal was then integrated to measure the angular excursion.

The IMU was placed on the instep of the (right) foot and attached snugly to the shoe with a Velcro strap, thus allowing secure fastening to the body part with minimal movement. As an alternative to this attachment method, the IMU can be also strapped under the shoelaces. Care was taken to locate the accelerometer sensitive axes in the sagittal plane; by sensor construction, the gyroscope sensitive axis was then perpendicular to this plane, so as to measure the angular velocity component that is parallel to the mediolateral axis. In some cases, two footswitches were also used as a reference standard to detect the gait events and to confirm the validity of the gait phase segmentation procedure. Each footswitch was composed of one pair of 10 mm-diameter Flexiforce force sensing resistors (Tekscan A201), connected in parallel to essentially act as one larger sensor and arranged in a voltage-divider configuration to indicate when weight was applied to them or not. One of the footswitches was placed underneath the heel and one underneath the big toe (right foot), and taped to the foot with some tape. Their outputs were digitized together with the IMU signals

( $f_s = 200 \text{ Hz}$ ). The time of heelstrike and toe-off was obtained by thresholding the footswitch outputs.

The main error sources affecting the response of inertial sensors are related to the effects of sensor uncertainty, namely offset, and sensitivity [23]. Other uncertainty sources are usually recognized as less important, including quantization noise involved in the analog-to-digital conversion, time discretization, and numerical errors incurred in the strapdown integration process. Of utmost importance to achieve accurate results in the estimate of the desired quantities is the care to be exercised to control the effect of the offset and sensitivity drifts, since they are functions of environmental conditions, e.g., ambient temperature, and are highly dependent on the characteristics of individual devices.

### B. Theory

The inertial coordinate system  $XYZ$  that is used to express foot orientation and position relative to the ground is represented in Fig. 1. The  $X$ -axis is defined in the direction of progression, the  $Z$ -axis vertically and the  $Y$ -axis perpendicular to the  $X$ - and  $Z$ -axes.

To simplify the experimental instrumentation and reduce the number of sensors, the main model assumption is that the leg motion is approximately planar, i.e., in the sagittal plane only. Accordingly, the pitch angle representing the IMU orientation  $\theta$  (negative clockwise) changes during walking. The accelerometer outputs  $a_x, a_z$  are modeled by projecting the foot acceleration  $\vec{a} = [a_x, a_z]^T$  and the gravitational acceleration  $\vec{g}$  along the corresponding sensitive axis. The components of  $\vec{a}$  can be, therefore, expressed as

$$a_X = a_x \cos \theta - a_z \sin \theta \quad (1a)$$

$$a_Z = a_x \sin \theta + a_z \cos \theta - g. \quad (1b)$$

The gyroscope signal is used to estimate the angular velocity  $\dot{\theta}$  around the  $Y$ -axis, and it is integrated to estimate  $\theta$ . The position of the sensed point on the foot instep is then obtained from the double-integration of (1a) and (1b). The sagittal orientation of the foot can be presented as the pitch angle (negative clockwise) relative to the reference orientation during stance; conversely, the coronal and frontal orientations are not considered in the following development.

### C. Data Analysis

Matlab v. 6.0 (The MathWorks) was used for off-line signal processing. A second-order forward-backward low-pass Butterworth filter was applied to sensor signals (cutoff frequency: 17 Hz, accelerometer signals; cutoff frequency: 15 Hz, gyroscope signal).

1) *Detection of Gait Events*: The function to gather information about the different gait phases is performed by the gyroscope. The procedure of segmentation divided the gait cycle into four phases: stance ( $ST$ ), heel-off ( $HO$ ), swing ( $SW$ ), heel-strike ( $HS$ ).

Suppose that the initial state occupied by the subject is  $ST$ , i.e., the subject is standing still in the upright posture—the foot is motionless. While in the  $ST$  state, the algorithm waits for the

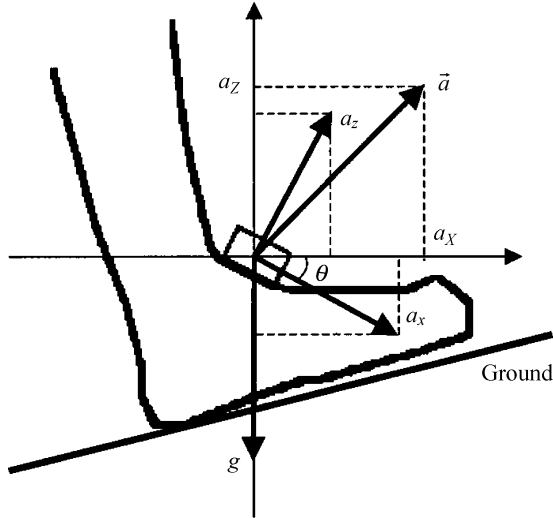


Fig. 1. Schematic representation of the measurement setup. The IMU is attached to the instep of the foot. The biaxial accelerometer, whose sensitive axes—assumed to lie in the vertical plane—are represented by arrows, measures the acceleration components  $a_x$ ,  $a_z$ . These components include contributions from the foot acceleration  $\vec{a} = [a_x, a_z]$  and the gravitational acceleration  $\vec{g}$ . The foot gyroscope measures the angular velocity around its sensitive axis, which is assumed to be orthogonal to the vertical plane, and allows to reconstruct the pitch angle  $\theta$  by integration. The knowledge of  $\theta$  is needed to remove the gravitational contribution from the accelerometer readings, before carrying the strapdown integration.

transition to the heel-off phase,  $T1 : ST - HO$ . It is assumed that the transition occurs when the condition

$$|\dot{\theta}| \geq TH_{HO} \quad (2)$$

is verified ( $TH_{HO}$  is a given threshold angular velocity,  $TH_{HO} = 30^\circ/s$ ). The time instant at which the transition takes place is retained as the heel-off time  $T_{HO}$ , and denotes the initial time  $T_{start}$  for the signal integration to start. Henceforth, all time instants are expressed in multiples of the system sampling interval  $T_s$ .

It is assumed that the transition  $T2 : HO - SW$  (the foot takes off) occurs at the time instant  $T_{TO}$  when the angular velocity reaches the maximum value in the clockwise direction. During the swing phase, the main feature appearing in the gyroscope signal is a rather broad positive pulse (counterclockwise rotation), whose peak value occurs, approximately, at the moment of mid-swing during the gait cycle. During late-swing, the angular velocity decreases.

It is assumed that the transition  $T3 : SW - HS$  (the foot contacts the ground) occurs at the time instant  $T_{HS}$  when the angular velocity reaches the maximum value in the clockwise direction for the second time in the gait cycle.

It is assumed that the transition  $T4 : HS - FF$  (the foot is flat on the ground) occurs when the condition

$$|\dot{\theta}| < TH_{FF} \quad (3)$$

is verified ( $TH_{FF}$  is a given threshold angular rate,  $TH_{FF} = 30^\circ/s$ ). Since the angular velocity is almost steady at  $0^\circ/s$ , the foot rolling phase is completed. The time instant  $T_{FF}$  when (3)

occurs denotes the final time  $T_{end}$  for the signal integration to end.

With reference to the  $j$ -th gait cycle, the estimators of the temporal gait parameters are as follows.

- Stride time,  $ST$ :

$$ST(j) = T_{HS}(j+1) - T_{HS}(j). \quad (4)$$

- Duration of the swing phase,  $T_{swing}$ :

$$T_{swing}(j) = T_{HS}(j+1) - T_{TO}(j). \quad (5)$$

- Duration of the stance phase,  $T_{stance}$ :

$$T_{stance}(j) = ST(j) - T_{swing}(j). \quad (6)$$

- Relative stance,  $RS$ :

$$RS(j) = \frac{T_{stance}(j)}{ST(j)} 100. \quad (7)$$

2) *Strapdown Integration*: The pitch angle is computed as follows:

$$\theta = INT \left[ \int_{T_{start}}^t \dot{\theta}(\tau) d\tau \right] + \theta_{init} \quad (8)$$

where  $INT[\cdot]$  denotes the rule for numerical approximation to the integral within brackets, e.g., the trapezoidal rule.  $\theta_{init}$  is computed by applying a variant of a “zero velocity update” technique [24]. It is based on averaging the angle from  $M$  accelerometer samples collected in the stance phase, when the accelerometers are exposed to the gravitational acceleration only

$$\theta_{init} = \frac{1}{M} \sum_{k=T_{start}-M}^{T_{start}} \tan^{-1}(a_x, a_z) \quad (9)$$

( $M = 25$ ). To improve the accuracy in the computation of (8), a nulling algorithm is applied to the gyroscope signal: it provides the offset estimate by averaging the angular velocity from  $N$  gyroscope samples ( $N = 100$ ) collected before subjects begin walking.

Since the features of human gait are cyclical, the foot inclination angle during stance is approximately constant from one gait cycle to the next one, unless abrupt slope variations are encountered during walking (not allowed, in the present context). Therefore, to remove the measurement error of the gyroscope due to electrical noise and sensor drift, the following resetting mechanism is applied

$$\hat{\theta}(i) = \theta(i) - \left[ \frac{i - T_{start}}{T_{end} - T_{start}} \right] [\theta(i) - \theta_{init}] \quad i = T_{start}, \dots, T_{end}. \quad (10)$$

The velocity components are computed as follows:

$$v_p = INT \left[ \int_{T_{start}}^t a_p(\tau) d\tau \right] + v_{p \text{ init}} \quad (11)$$

$p = X, Z$ —see (1a) and (1b), where the pitch angle is  $\hat{\theta}(i)$ . Since the foot is motionless at the time instant  $T_{\text{start}}$ , the initial condition is  $v_p \text{init} = 0$ . Finally, to remove the measurement error of the accelerometers and gyroscope due to electrical noise and sensor drift, the following resetting mechanism is applied:

$$\hat{v}_p(i) = \left( \frac{T_{\text{end}} - i}{T_{\text{end}} - T_{\text{start}}} \right) v_p(i) \quad i = T_{\text{start}}, \dots, T_{\text{end}}. \quad (12)$$

The displacement components can be computed as follows:

$$d_p = INT \left[ \int_{T_{\text{start}}}^t \hat{v}_p(\tau) d\tau \right] + \sum_{k=1}^{j-1} d_p(T_{\text{end}}(k)) \quad (13)$$

where the initial condition reflects the total displacement summed over the  $j - 1$  gait cycles since the beginning of the walking trial (for  $j = 1$ ,  $d_p \text{init} = 0$ ). The path travelled during the  $j$ -th gait cycle can be decomposed into two distinct components

$$D_X(j) = d_X(T_{\text{end}}(j)) - \sum_{k=1}^{j-1} d_X(T_{\text{end}}(k)) \quad (14a)$$

$$D_Z(j) = d_Z(T_{\text{end}}(j)) - \sum_{k=1}^{j-1} d_Z(T_{\text{end}}(k)) \quad (14b)$$

which allows to compute the horizontal and vertical (average) speed components

$$\begin{aligned} V_X(j) &= \frac{D_X(j)}{[T_{\text{start}}(j+1) - T_{\text{start}}(j)]} \\ V_Z(j) &= \frac{D_Z(j)}{[T_{\text{start}}(j+1) - T_{\text{start}}(j)]}. \end{aligned} \quad (15)$$

Finally, the stride length  $SL$ , the walking speed  $V$  and the incline  $I$  are

$$\begin{aligned} SL(j) &= \sqrt{D_X^2(j) + D_Z^2(j)} \\ V(j) &= \frac{SL(j)}{[T_{\text{start}}(j+1) - T_{\text{start}}(j)]} \\ I(j) &= \left( \frac{D_Z(j)}{D_X(j)} \right) 100. \end{aligned} \quad (16)$$

#### D. Experimental Method

The subjects were five healthy adult males without any history of orthopedic or neuromuscular impairments (age:  $30 \pm 7$  years, height:  $1.80 \pm 0.06$  m, weight:  $79 \pm 7$  kg), who had given informed consent prior to participation. The walking experiments were performed using a motor-driven treadmill (Technogym, Runrace HC1200), in which speed and incline could be adjusted and controlled. The treadmill was successfully calibrated by comparing the nominal speed  $V_t$  and the incline  $I_t$  with separately measured values of these variables.

The IMU was calibrated before each experimental session. When the IMU was attached to the (right) foot, the norm of the acceleration vector was  $1g$ , i.e., the accelerometer sensitive axes were approximately parallel to the sagittal plane. Before each

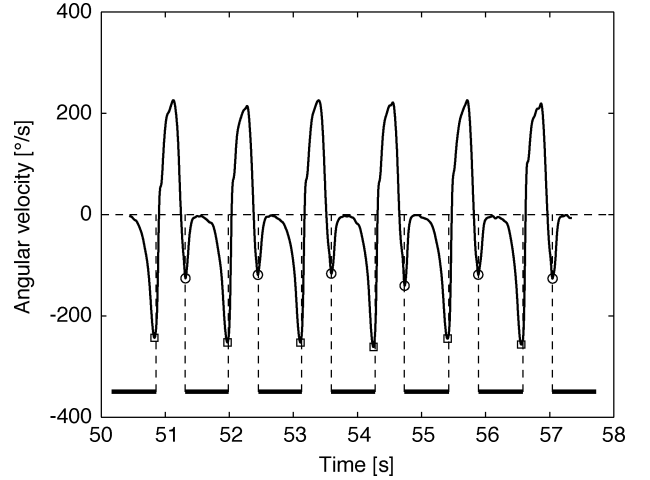


Fig. 2. Estimation of toe-off (□) and heelstrike (O) obtained from applying the detection algorithm to the foot gyroscope signal. The gait phases detected by the toe and heel footswitches are also reported to show their correspondence with the patterns of angular velocity.

walking trial, the pitch angle was checked, beside the  $1g$ -condition. This was done to detect significant movements of the IMU relative to the foot throughout the experimental session.

Subjects were given sufficient time to familiarize with treadmill walking before starting with the experiments, during which they wore their own gym shoes. Seven walking speeds from 3 km/h to 6 km/h in steps of 0.5 km/h were selected at each of the five inclines:  $-5\%$ ,  $0\%$ ,  $5\%$ ,  $10\%$ , and  $15\%$ . For each combination of speed and incline, subjects were asked to walk at their normal pace for a period of 2 min; resting periods of 2 min were allowed between successive trials.

Data from the gait cycles inside the interval  $[50, 110]$  s of each trial were used to compute the means  $V_m$ ,  $I_m$ , and  $RS_m$  and the standard deviations of  $V$ ,  $I$ , and  $RS$ . The relationship connecting  $RS_m$  to  $V_t$  and  $I_t$  was analyzed using standard regression tools.  $V_m$  and  $I_m$  were compared with  $V_t$  and  $I_t$ , respectively, to assess the accuracy of the proposed measuring method in terms of root mean square errors (RMSEs).

### III. RESULTS

A typical example of foot angular velocity during six consecutive gait cycles is plotted in Fig. 2; the temporal events detected by the footswitches, i.e., toe-off and heelstrike are also represented, to show their correspondence with the features appearing in the gyroscope signal.

Averaged measurements of 300 gait cycles at varying speeds and inclines from two subjects indicate that the foot gyroscope measuring method tends to detect the toe-off earlier (on average: 35 ms), whilst the heelstrike is detected without any systematic difference (on average:  $-2$  ms, confidence interval at 95%:  $[-16, 12]$  ms), as compared with the footswitch measuring method.

The  $RS$  values are not significantly influenced by the incline. The relationship between  $RS_m$  (averaged across subjects and

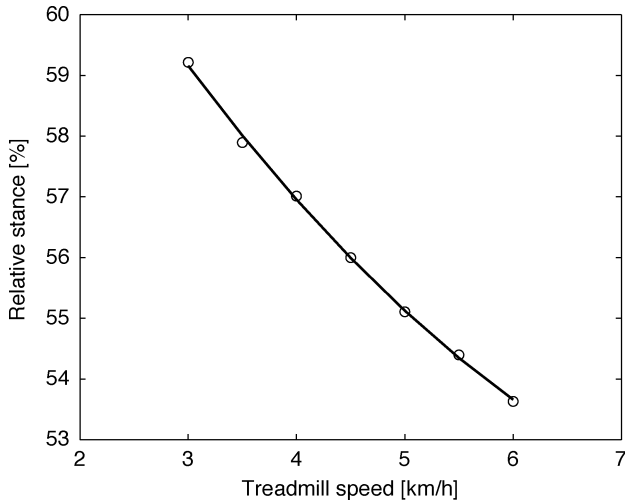


Fig. 3. Relationship between estimated relative stance and treadmill speed. At each speed, the data are averaged across inclines and tested subjects. Superimposed to the data, the regression curve constructed from a second-order polynomial model, see text.

inclines) and  $V_t$  is reported in Fig. 3 ( $RS_{\bar{m}} = 0.18V_t^2 - 3.49V_t + 67.98$ ,  $r^2 > 0.99$ ).

The foot angular velocity and the offset-corrected sagittal orientation of the foot are shown in Fig. 4, for three consecutive gait cycles from a walking trial carried at  $V_t = 4$  km/h,  $I_t = 0\%$ .

Other kinematic traces of interest, i.e., the horizontal and vertical acceleration and the corresponding drift-corrected velocity components  $\hat{v}_p$  are related to the three gait cycles represented in Fig. 4 and are shown in Figs. 5 and 6.

The reconstructed trajectory of the foot point which the IMU is attached to is plotted in Fig. 7.

Typical results obtained during 1 min of a walking trial carried at  $V_t = 4$  km/h,  $I_t = 0\%$  are presented in Fig. 8.

Table I yields the uncertainty in the speed and incline estimates for each subject.

The relationship between estimated speed  $\hat{V}_m$  (averaged across subjects and inclines) and  $V_t$  is constructed in Fig. 9 ( $\hat{V}_m = 0.936V_t + 0.173$ ,  $r^2 > 0.99$ ); the relationship between estimated incline  $\hat{I}_m$  (averaged across subjects and speeds) and  $I_t$  is constructed in Fig. 10 ( $\hat{I}_m = 0.851I_t + 0.371$ ,  $r^2 > 0.99$ ).

The overall uncertainty in the speed and incline estimates is  $RMSE = 0.18$  km/h (0.05 m/s) and  $RMSE = 1.52\%$ , respectively. When the analysis is restricted to incline  $-5\%$ ,  $0\%$ ,  $5\%$ ,  $10\%$  the estimation uncertainty decreases:  $RMSE = 1.09\%$ ; the linear regression function explaining the relationship between  $\hat{I}_m$  and  $I_m$  becomes:  $\hat{I}_m = 0.907I_m + 0.371$ ,  $r^2 > 0.99$ . The coefficient of variation ( $CV$ ) affecting  $V_m$  is  $CV = 4\%$ . The standard error ( $SE$ ) affecting  $I_m$  is  $SE = 6\%$ , i.e., the standard deviation is  $1.2\%$  over the full range  $[-5, +15]\%$ .

#### IV. DISCUSSION

Compared with the reference standard based on footswitches, relatively small temporal changes are detected when the gait phase segmentation procedure adheres to the approach proposed in [11]. As compared to the latter, we do not use wavelet based enhancements techniques. They find that the shank gyroscope detects the toe-off without any significant temporal

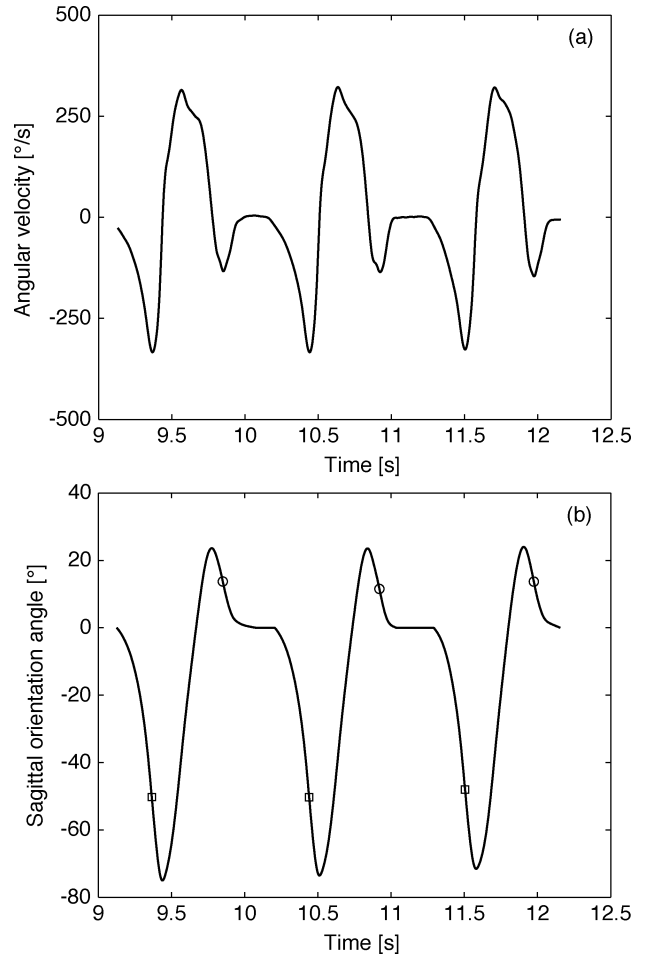


Fig. 4. Three consecutive gait cycles, showing the foot gyroscope signal (a), and the sagittal orientation of the foot, after integration and resetting (b)  $-V_t = 4$  km/h,  $I_t = 0\%$ . The initial condition (during stance) is estimated from the accelerometric readings, see text. The sagittal orientations of the foot before toe-off ( $\square$ ) and heelstrike ( $\circ$ ) are also indicated. According to the sign convention adopted in this paper (pitch angles are negative clockwise), a negative sagittal orientation corresponds to a foot posture where the toe height exceeds the heel height relative to the ground; a null sagittal orientation means that the foot is flat relative to the ground.

change compared with the footswitches, whilst the heelstrike detection is affected by a small systematic delay (on average: 10 ms). Conversely, we find that the toe-off detection by the foot gyroscope is slightly biased (on average: 35 ms), whilst the heelstrike is not. Beside [11], two other studies have previously investigated the correspondence between gait events and the gyroscope angular velocity [2], [10]. The measuring method proposed in [10] exploits one shank gyroscope to perform toe-off detection, leading to the same conclusion as in [11]. In [2] it is proposed to use a heel gyroscope and three footswitches located underneath the heel, first and fourth heads of the metatarsal bones. The heelstrike is detected by the heel footswitch; the toe-off is identified by the change of sign in the angular velocity signal after heel-off, provided that the footswitches are not pressed. Compared with the reference standard based on an optical motion analysis system, it is concluded that, on average, the heelstrike and toe-off detections are affected by systematic delays of approximately 70 and 35 ms, respectively. Note that the pattern of angular velocity appearing in Fig. 2 is very similar to that reported in [2]. Since the heel

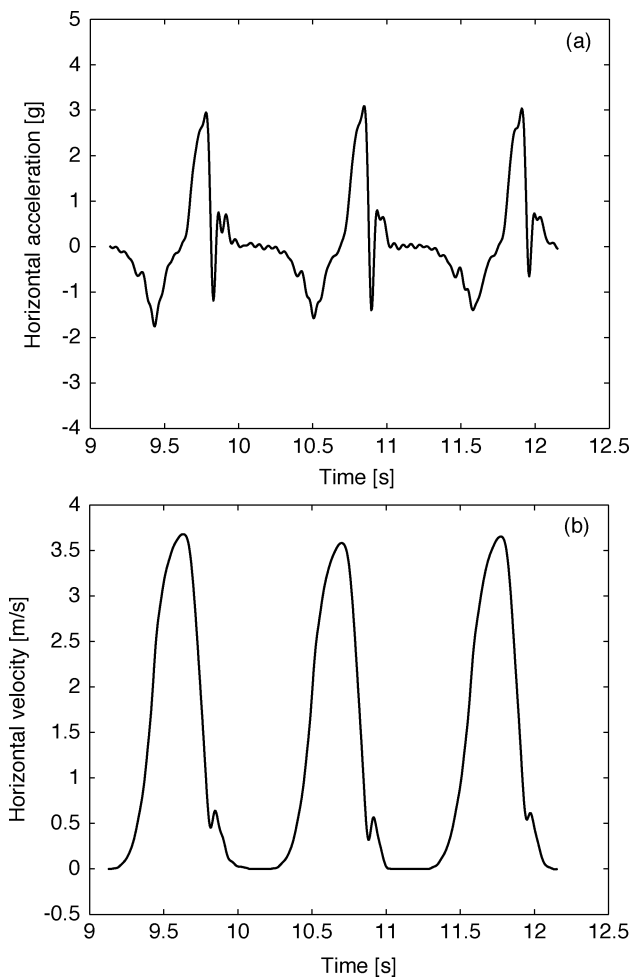


Fig. 5. With reference to the same gait cycles as in Fig. 4, the horizontal component of foot acceleration  $a_X$  (a), and the reconstructed velocity component  $v_X$  after integration and resetting (b). The initial condition (during stance) is null, see text.

and the instep of the foot are submitted to similar movement patterns around the ankle joint, similar signal patterns are to be expected from heel and foot gyroscopes; the consequence is that their zero-crossings after heel-off are highly correlated—compared with the footswitches, the systematic delay of the zero-crossing after heel-off computed on the signals from the foot gyroscope turns out to be approximately 55 ms. However, it should be noted that the detection of gait events by footswitches is critically dependent on the choice of the threshold level to be applied to their output signals: hence, small differences may be accounted for by different threshold settings.

Additional results come from the temporal analysis and are discussed in terms of the relative stance behavior: the across-subject averaged  $RS$  estimates are not significantly influenced by the incline, for a given walking speed; additionally, they tend to decrease with the speed, with overall variations in the interval [54%, 59%]. These results are consistent with known facts about the biomechanics of normal walking. First, the average  $RS$  values are approximately 60% for normal overground walking at self-selected speed; however, the results reported in [25] indicate average  $RS$  values around 58% for normal tread-

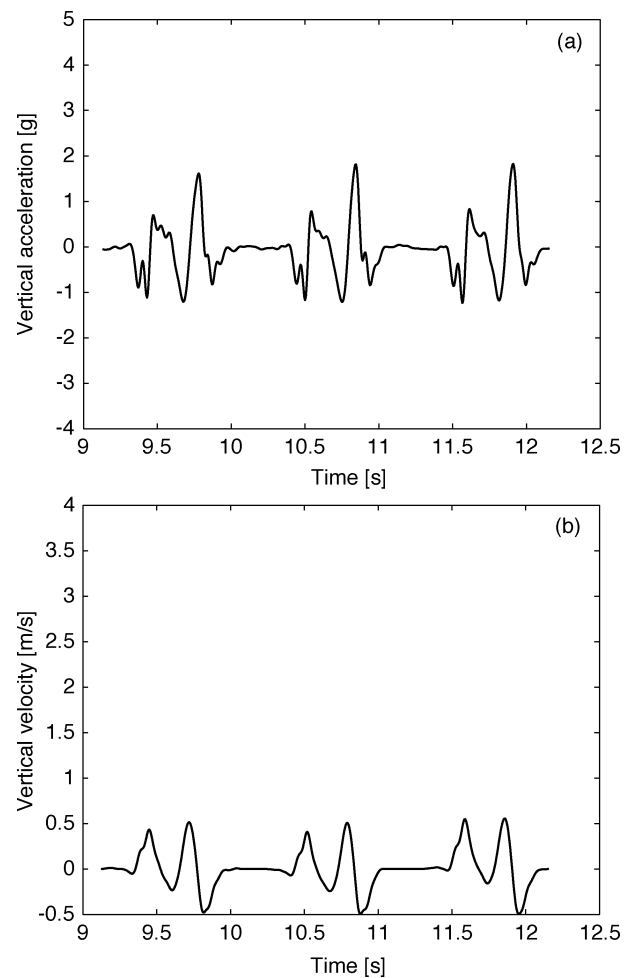


Fig. 6. With reference to the same gait cycles as in Fig. 4, the vertical component of foot acceleration  $a_Z$  (a), and the reconstructed velocity component  $v_Z$  after integration and resetting (b). The initial condition (during stance) is null, see text.

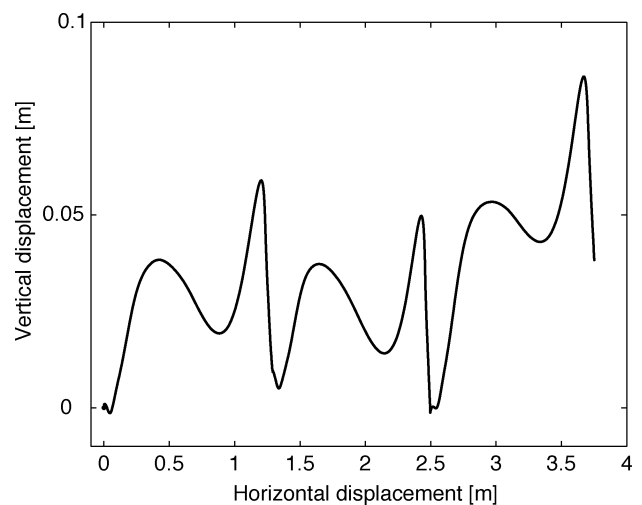


Fig. 7. With reference to the same gait cycles as in Fig. 4, the reconstructed trajectory in the sagittal plane of the sensed point on the foot instep, after integration of both  $v_X$  and  $v_Z$ .

mill walking at self-selected speed, i.e., treadmill walking is characterized by a slightly longer aerial phase than overground walking. Second, it is known that, during treadmill walking, the

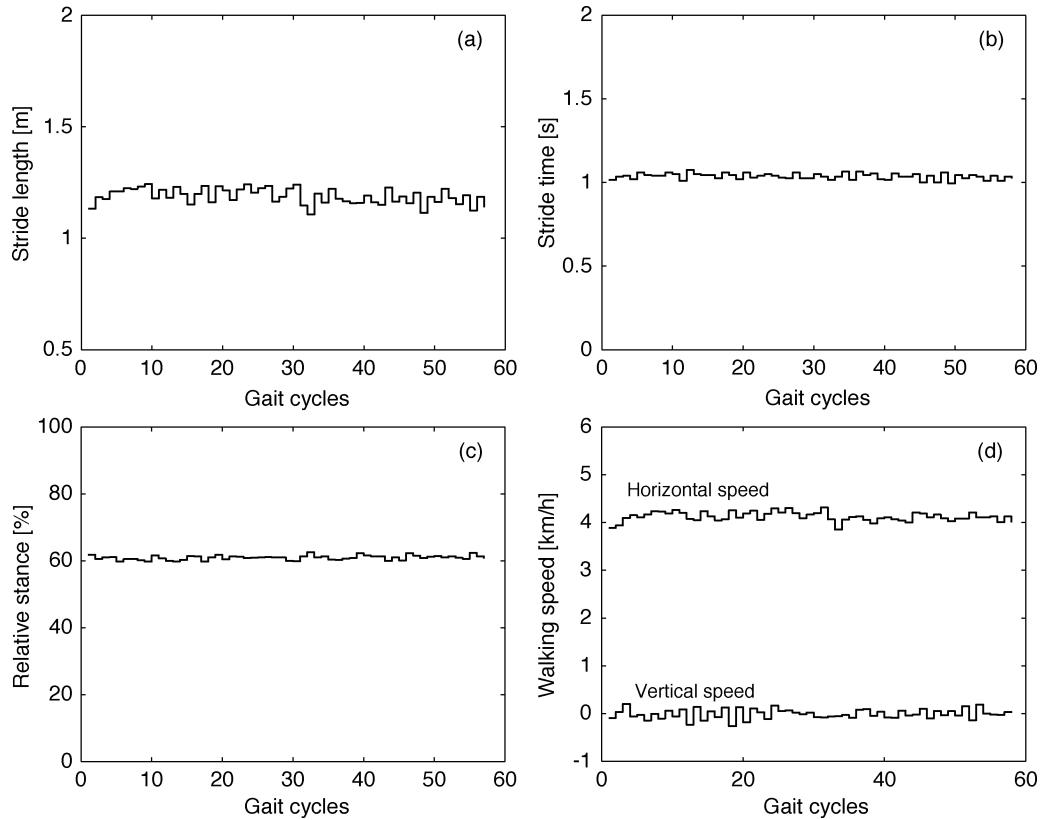


Fig. 8. Stride length, stride time, relative stance, and walking speed, decomposed in its estimated horizontal and vertical components obtained from one subject during 1 min of treadmill walking ( $V_t = 4$  km/h,  $I_t = 0\%$ ). These estimates, constructed at each gait cycle, are helpful to analyze the joint effect of measurement errors and stride variability.

TABLE I  
THE UNCERTAINTY AFFECTING THE SPEED AND INCLINE ESTIMATES IS REPORTED IN TERMS OF THE COMPUTED RMSE VALUES FOR EACH SUBJECT

	S1	S2	S3	S4	S5
Speed [km/h]	0.18	0.12	0.20	0.22	0.10
Incline [%]	1.75	1.53	1.33	1.34	1.11

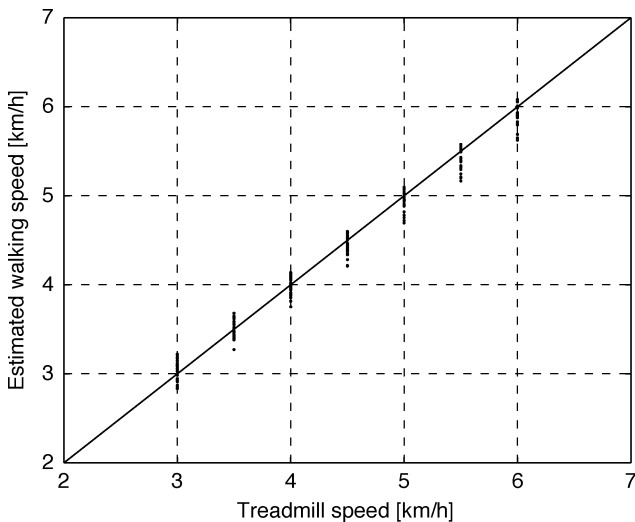


Fig. 9. Relationship between estimated walking speed and treadmill speed for all inclines and tested subjects. The line represents the identity line.

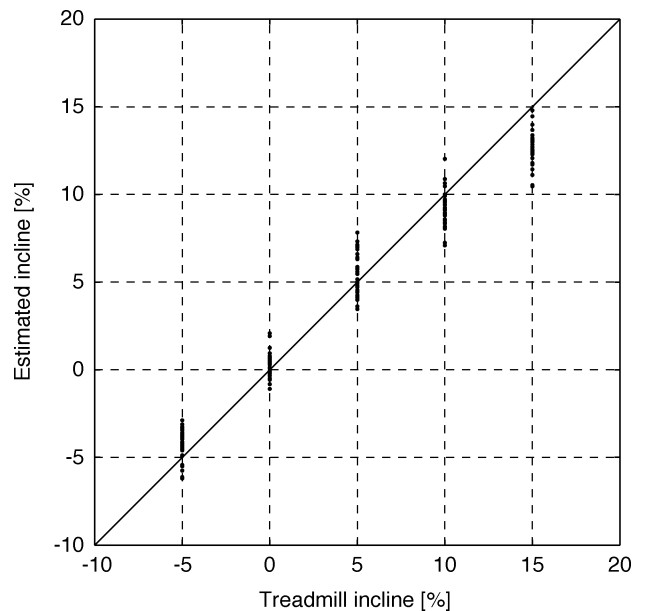


Fig. 10. Relationship between estimated incline and treadmill incline for all speeds and tested subjects. The line represents the identity line.

proportion of stance and swing phases relative to cycle duration

is not affected by the change in slope, but tends to decrease with speed [26], [27].

The cyclical qualities of gait are used to drive the strap-down integration, see Figs. 4–7. The accuracy in determining the sagittal orientation of the foot and the position of the anatomical sensed point is critically dependent on the inertial

sensor performance, e.g., offset, sensitivity drift, range, on the validity of the biomechanical assumption of planar leg motion, and on the effects of relative movements between the shoe-mounted IMU case and the skeleton structure underneath (sensor jolting).

The accelerometric information content during stance is beneficial in removing the uncertainty in the initial conditions of the pitch angle. The resetting algorithm aims at preventing the unbounded growth of integration errors due to low-frequency noise, i.e., sensor offset and sensitivity drift, by limiting the duration of the strapdown integration intervals to single gait periods. The resetting technique cannot be applied to the integration of the velocity components in (14a), (14b), unless the incline is *a priori* known to be zero at the  $j$ -th gait cycle (level walking), in which case, necessarily,  $d_z(T_{\text{end}}(j)) = d_z(T_{\text{start}}(j)) = 0$  in (14b). Because of this, low-frequency noise can influence the reconstructed trajectory, as outlined in Fig. 8, which concerns gait cycles during treadmill walking at incline 0%.

As for the adequacy of the planar gait model, a 3-D inertial sensing system would relax these assumptions by wholly accounting for the subtle complexity of the foot motion. The absolute accuracy of our reduced-complexity approach is yet to be compared with, e.g., a 3-D motion analysis system.

At the present time, no indication is available in the literature as to the influence of relative movements between a shoe-mounted, or a skin-mounted, sensor case and the skeleton structure underneath on the accuracy achieved by strapdown integration; there exists some evidence that the assumption of rigid-body condition is predominant in determining the accuracy of angle measurements with accelerometers [28], and that skin-mounted accelerometers may distort the acceleration profiles with respect to bone-mounted accelerometers [29]. We cannot rule out the possibility that movements of the IMU relative to the skeleton structure may occur in our application, particularly at the ground impact. Sensor attachment by strapping the IMU case to the foot instep—the attachment method used in this paper—is used in [20], [21], where applications related to walking are studied. This attachment method is likely to be not wholly satisfactory during running and jumping. The best way to deal with the sensor attachment problem in the latter applications can be by means of “mechanical stabilizers,” such as those described, for instance, in [30], where the authors deal with the design of instrumented shoes for dancers.

With regard to sensor jolting, it is worthy noting that the pitch angle and the 1  $g$ -condition during stance turn out to be quite stable in our experiments: in particular, the intrasubject variability of the pitch angle estimated during the “standing still” phase on the treadmill belt amounts to about 1.2° standard deviation over the duration of the whole experimental session (approximately, a couple of hours). Additionally, adequate filtering is applied to attenuate the high-frequency noise components added to the output of both accelerometers and gyroscope which may be due to sensor jolting [4].

We can provide a reasonable assessment of the influence of the mentioned error sources by comparing the walking speed and incline estimates with their nominal values—see the typical example in Fig. 8. The achieved measurement accuracy is re-

markable and favorably compares with competing approaches [6], [11]. In our data, it is observed that a performance degradation occurs at the steepest incline, see Figs. 9 and 10: also, the regression analysis indicates that both walking speed and incline turn out to be slightly underestimated. This fact can be explained as the sign of limitations in sensor range. Foot acceleration peak values are less than 5  $g$  in an interval of walking speeds similar to ours; in the same conditions, foot angular velocities with peak values as high as 650°/s peak at toe-off and 300°/s at mid-swing are measured, whilst peak values of about 400°/s at mid-swing are reported for the shank (average speed: 4.8 km/h) [31]. Since the full range of the accelerometers is  $\pm 10 g$ , the foot accelerometers would not suffer from range limitations. Conversely, the foot angular velocities can exceed the limit of  $\pm 300^\circ/\text{s}$  indicated in the Murata technical literature as the *maximum* angular velocity range [32]. The increase in foot angular velocity with walking speed would have another effect on the system performance, since the stance phase becomes increasingly short; as a consequence, it is increasingly difficult to reliably reset the strapdown integrals. Since the shank is continuously rotating over the foot during the gait cycle, it is reasonable to expect that the shank gyroscope is more affected by this difficulty than the foot gyroscope, although the discussed range limitation is likely to have a heavier influence on the foot gyroscope. We believe that it is unlikely that the sensor range limitations can influence the performance of the gait phase segmentation procedure, unless the sensor output signals are saturated, condition we have never observed in our signals.

## V. CONCLUSION

In this paper, we have presented an ambulatory monitoring system intended for the estimation of several spatio-temporal parameters of gait. The system, built around a simple IMU placed on the foot, gathers information about the occurrences of different gait events (heel-off, toe-off, heelstrike, foot-flat) and reconstructs the sagittal trajectory of the sensed anatomical point—the instep of the foot—, yielding information about walking speed and incline. Although tested so far during treadmill walking only, the ambulatory monitoring system shows remarkable accuracy when compared to state-of-the-art systems tested in similar conditions. We conclude that foot inertial sensing is a promising measuring method for which several applications in rehabilitation, sport medicine, health monitoring can be considered and are planned in our research agenda.

## REFERENCES

- [1] Y. Ohtaki, K. Sagawa, and H. Inooka, “A method for gait analysis in a daily living environment by body-mounted instruments,” *JSME Int. J.*, vol. 44, no. 4, pp. 1125–1132, 2001.
- [2] I. P. I. Pappas, M. R. Popovic, T. Keller, V. Dietz, and M. Morari, “A reliable gait phase detection system,” *IEEE Trans. Rehab. Eng.*, vol. 9, no. 2, pp. 113–125, Jun. 2001.
- [3] P. H. Veltink, H. B. J. Bussmann, W. de Vries, W. L. J. Martens, and R. C. Van Lummel, “Detection of static and dynamic activities using uniaxial accelerometers,” *IEEE Trans. Rehab. Eng.*, vol. 4, no. 4, pp. 375–385, Dec. 1996.



- [4] C. V. C. Bouten, K. T. M. Koekoek, M. Verduin, R. Kodde, and J. D. Janssen, "A triaxial accelerometer and portable data processing unit for the assessment of daily physical activity," *IEEE Trans. Biomed. Eng.*, vol. 44, no. 3, pp. 136–147, Mar. 1997.
- [5] J. B. J. Bussmann, P. H. Veltink, F. Koelma, R. C. Van Lummel, and H. J. Stam, "Ambulatory monitoring of mobility-related activities: the initial phase of the development of an activity monitor," *Eur. J. Phys. Med. Rehab.*, vol. 5, no. 1, pp. 2–7, 1995.
- [6] K. Aminian, P. Robert, E. Jéquier, and Y. Schutz, "Incline, speed, and distance assessment during unconstrained walking," *Med. Sci. Sports Exerc.*, vol. 27, pp. 226–234, 1995.
- [7] K. Aminian, K. Rezakhanlou, E. D. Andres, C. Fritsch, P.-F. Leyvraz, and P. Robert, "Temporal feature estimation during walking using miniature accelerometers: an analysis of gait improvement after hip arthroplasty," *Med. Biol. Eng. Comput.*, vol. 37, pp. 686–691, 1999.
- [8] A. L. Evans, G. Duncan, and W. Gilchrist, "Recording accelerations in body movements," *Med. Biol. Eng. Comput.*, vol. 29, pp. 102–104, 1991.
- [9] S. Miyazaki, "Long-term unrestrained measurement of stride length and walking velocity utilizing a piezoelectric gyroscope," *IEEE Trans. Biomed. Eng.*, vol. 44, no. 8, pp. 753–759, Aug. 1997.
- [10] K. Tong and M. H. Granat, "A practical gait analysis system using gyroscopes," *Med. Eng. Phys.*, vol. 21, no. 1, pp. 87–94, 1999.
- [11] K. Aminian, B. Najafi, C. Büla, P.-F. Leyvraz, and P. Robert, "Spatio-temporal parameters of gait measured by an ambulatory system using miniature gyroscopes," *J. Biomech.*, vol. 35, pp. 689–699, 2002.
- [12] O. Perrin, P. Terrier, Q. Ladetto, B. Merminod, and Y. Schutz, "Improvement of walking speed prediction by accelerometry and altimetry, validated by satellite positioning," *Med. Biol. Eng. Comput.*, vol. 38, pp. 164–168, 2000.
- [13] P. Terrier, Q. Ladetto, B. Merminod, and Y. Schutz, "High-precision satellite positioning system as a new tool to study the biomechanics of human locomotion," *J. Biomech.*, vol. 33, pp. 1717–1722, 2000.
- [14] R. Moe-Nilssen, "A new method for evaluating motor control in gait under real-life environmental conditions. Part I: the instrument," *Clin. Biomech.*, vol. 13, pp. 320–327, 1998.
- [15] J. R. Morris, "Accelerometry—a technique for the measurement of human body movements," *J. Biomech.*, vol. 6, pp. 729–736, 1973.
- [16] A. T. M. Willemsen, F. Bloemhof, and H. B. K. Boom, "Automatic stance-swing phase detection from accelerometer data for peroneal nerve stimulation," *IEEE Trans. Biomed. Eng.*, vol. 37, no. 12, pp. 1201–1208, Dec. 1990.
- [17] R. E. Mayagoitia, A. V. Nene, and P. H. Veltink, "Accelerometer and rate gyroscopes measurement of kinematics: an inexpensive alternative to optical motion analysis systems," *J. Biomech.*, vol. 35, pp. 537–542, 2002.
- [18] R. Williamson and B. J. Andrews, "Detecting absolute human knee angle and angular velocity using accelerometers and gyroscopes," *Med. Biol. Eng. Comput.*, vol. 39, pp. 294–302, 2001.
- [19] J. E. Bortz, "A new mathematical formulation for strapdown inertial navigation," *IEEE Trans. Aerosp. Electron. Syst.*, vol. AE-7, pp. 61–66, 1971.
- [20] P. H. Veltink, P. Slycke, J. Hemssems, R. Buschman, G. Bulstra, and H. Hermens, "Three dimensional inertial sensing of foot movements for automatic tuning of a two-channel implantable frop-foot stimulator," *Med. Eng. Phys.*, vol. 25, no. 1, pp. 21–28, 2003.
- [21] K. Sagawa, Y. Sato, and H. Inooka, "Non-restricted measurement of distance during level walk," *Trans. Soc. Instrum. Control Eng.*, vol. 36, no. 11, pp. 909–915, 2000.
- [22] K. Sagawa, H. Inooka, and Y. Satoh, "Non-restricted measurement of walking distance," in *Proc. IEEE Int. Conf. Systems, Man, and Cybernetics*, vol. 3, 2000, pp. 1847–1852.
- [23] F. Ferraris, U. Grimaldi, and M. Parvis, "Procedure for effortless in-field calibration of three-axis rate gyros and accelerometers," *Sensors Mater.*, vol. 7, no. 5, pp. 311–330, 1995.
- [24] C. Verplaetse, "Inertial proprioceptive devices: self-motion-sensing toys and tools," *IBM Syst. J.*, vol. 35, no. 3/4, pp. 639–650, 1996.
- [25] H. Stolze, J. P. Kuitz-Buschbeck, C. Mondwurf, A. Boczek-Funcke, K. Jöhnk, G. Deuschl, and M. Illert, "Gait analysis during treadmill and overground locomotion in children and adults," *Electroencephalogr. Clin. Neurophysiol.*, vol. 105, pp. 490–497, 1997.
- [26] K. Kawamura, A. Tokuhira, and H. Takechi, "Gait analysis of slope walking: a study on step length, stride width, time factors and deviation in the center of pressure," *Acta Med. Okayama*, vol. 45, no. 3, pp. 179–184, 1991.
- [27] A. Leroux, J. Fung, and H. Barbeau, "Postural adaptation to walking on inclined surfaces: I. Normal strategies," *Gait Posture*, vol. 15, no. 1, pp. 64–74, 2002.
- [28] A. T. M. Willemsen, C. Frigo, and H. B. K. Boom, "Lower extremity angle measurement with accelerometers—error and sensitivity analysis," *IEEE Trans. Biomed. Eng.*, vol. 38, no. 12, pp. 1186–1193, Dec. 1991.
- [29] M. A. Lafortune, "Three-dimensional acceleration of the tibia during walking and running," *J. Biomech.*, vol. 24, no. 10, pp. 877–886, 1991.
- [30] J. A. Paradiso, K. Hsiao, A. Y. Benbasat, and Z. Teegarden, "Design and implementation of expressive footwear," *IBM Syst. J.*, vol. 39, no. 3/4, pp. 511–529, 2000.
- [31] G. Wu and Z. Ladin, "The study of kinematic transients in locomotion using the integrated kinematic sensor," *IEEE Trans. Rehab. Eng.*, vol. 4, no. 3, pp. 193–200, Sep. 1996.
- [32] Product Engineering Section, Murata MFG. Co., Ltd., Kyoto, Japan, Operation Manual of Gyrostar, 1999.



**Angelo M. Sabatini** (M'90) received the Dr. Eng. degree in electrical engineering from the University of Pisa, Pisa, Italy, in 1986, and the Ph.D. degree in biomedical robotics from Scuola Superiore Sant'Anna, Pisa, in 1992.

From 1987–1988 he was with Centro E. Piaggio, Faculty of Engineering, University of Pisa. During the summer of 1988, he was a Visiting Scientist at the Artificial Organ Lab, Brown University, Providence, RI. From 1991–2001, he was an Assistant Professor of Biomedical Engineering at Scuola

Superiore Sant'Anna, where he has been an Associate Professor of Biomedical Engineering since 2001. His main research interests are: design and validation of intelligent assistive devices and wearable sensor systems, biomedical signal processing and quantification of human performance.



**Chiara Martelloni** graduated in biomedical engineering from the University of Pisa, Pisa, Italy, in 2002.

Since then, she has been a research fellow at Scuola Superiore Sant'Anna, Pisa. Her field of research includes wearable sensors, movement analysis, and biomedical signal processing.



**Sergio Scapellato** was born in Augusta, Siracusa, Italy, in 1977. He received the degree in electronic engineering (Diploma di Laurea) from the University of Pisa, Pisa, Italy, in 2002. He is currently working towards the Ph.D. degree in technology of sensor networking at Scuola Superiore Sant'Anna, Pisa.

From January to December 2003, he was a Research Fellow at Scuola Superiore Sant'Anna, Pisa. His field of research includes sensor networking, inertial sensing, movement analysis, and biomedical signal processing.



**Filippo Cavallo** received the degree in electronic engineering (Diploma di Laurea) from the University of Pisa, Pisa, Italy, in 2003. He is currently working towards the Ph.D. degree in pedestrian navigation at Scuola Superiore Sant'Anna, Pisa.

From March to December 2003, he was a Research Fellow at Scuola Superiore Sant'Anna, Pisa. His field of research includes wearable sensor systems, sensor networking, and GPS navigation.